The Journal of Nutrition
Nutrition and Disease

Distinct Adipose Depots from Mice Differentially Respond to a High-Fat, High-Salt Diet[1–3]

Vanessa C DeClercq,[4,8] Jennifer S Goldsby,[4] David N McMurray,[4,7] and Robert S Chapkin[4–7]*

[4]Program in Integrative Nutrition and Complex Diseases, [5]Department of Nutrition and Food Science, and [6]Center for Translational Environmental Health Research, Texas A&M University, College Station, TX; and [7]Department of Microbial Pathogenesis and Immunology, School of Medicine, Texas A&M University Health Science Center, College Station, TX

Abstract

Background: Dietary factors such as high-sodium or high-fat (HF) diets have been shown to induce a proinflammatory phenotype. However, there is limited information with respect to how microenvironments of distinct intra-abdominal adipose depots respond to the combination of a high-salt, HF diet.

Objective: We tested the hypothesis that HF feeding would cause changes in distinct adipose depots, which would be further amplified by the addition of high salt to the diet.

Methods: Twenty-seven male C57BL6 mice were fed an HF diet (60% of kcal from fat), an HF + high-salt diet (4% wt:wt), a control diet [low-fat (LF);10% of kcal from fat], or an LF + high-salt diet for 12 wk. The main sources of fat in the diets were corn oil and lard. Adipokines in serum and released from adipose tissue organ cultures were measured by immunoassays. QIAGEN's Ingenuity Pathway Analysis was used to perform functional analysis of the RNA-sequencing data from distinct adipose depots.

Results: Diet-induced obesity resulted in a classical inflammatory phenotype characterized by increased concentrations of circulating inflammatory mediators (38–56%) and reduced adiponectin concentrations (27%). However, high-salt feeding did not exacerbate the HF diet–induced changes in adipokines and cytokines. Leptin and interleukin-6 were differentially released from adipose depots and HF feeding impaired adiponectin and resistin secretion across all 3 depots (34–48% and 45–83%, respectively). The addition of high salt to the HF diet did not further modulate secretion in cultured adipose tissue experiments. Although gene expression data from RNA sequencing indicated a >4.3-fold upregulation of integrin αX (*Itgax*) with HF feeding in all 3 depots, markers of cellular function were differentially expressed in response to diet across depots.

Conclusion: Collectively, these findings highlight the role of distinct adipose depots in mice in the development of obesity and emphasize the importance of selecting specific depots to study the effects of therapeutic interventions on adipose tissue function. *J Nutr* 2016;146:1189–96.

Keywords: adipose depots, obesity, high fat/salt diet, adipokines, RNA-sequencing

Introduction

Excess delivery of nutrients to adipose tissue in obesity results in an increase in adipose tissue mass, followed by an increase in immune cells and thereby an altered production of proinflammatory adipokines, ultimately contributing to the progression of chronic inflammation (1, 2). Studies indicate differences in gene expression between adipose tissue depots in different anatomic locations, particularly between visceral and subcutaneous depots (3, 4). Thus, depots may be differentially influenced by the influx of distinct immune cell populations. Cohen et al. (5) suggested that different visceral adipose depots should not be considered interchangeable and showed that distinct adipose depots from lean mice have unique immune cell microenvironments. However, there is limited information on changes in immune cell populations and secretory function in different adipose depots during obesity, particularly between different visceral depots that may be influenced by dietary stimulants.

Associations between sodium intake and adiposity have been reported in humans (6–8), and short-term increases in dietary salt intake have been shown to activate a proinflammatory phenotype in monocytes (9). Obese mice fed high-sodium diets

[1] Supported by NIH R35CA197707, RO1CA168312, and P30ES023512.
[2] Author disclosures: VC DeClercq, JS Goldsby, DN McMurray, and RS Chapkin, no conflicts of interest.
[3] Supplemental Tables 1–3, Supplemental Figures 1 and 2, Supplemental Methods, and Supplemental References are available from the "Online Supporting Material" link in the online posting of the article and from the same link in the online table of contents at http://jn.nutrition.org.
[8] Present address: Department of Biochemistry and Molecular Biology, Dalhousie University, Halifax, Nova Scotia, Canada.
*To whom correspondence should be addressed. E-mail: r-chapkin@tamu.edu.

Manuscript received November 23, 2015. Initial review completed January 11, 2016. Revision accepted March 22, 2016.
First published online May 4, 2016; doi:10.3945/jn.115.227496.

not only gained more weight but exhibited increased inflammatory *Il6*, monocyte chemotactic protein 1 (*Mcp1*)[9], and tumor necrosis factor (*Tnf*) mRNA and lower adiponectin mRNA expression than mice fed low-sodium diets (10). In addition, high-fat (HF) feeding alone in mice has been shown to cause an increase in proinflammatory, classically activated macrophages (M1) (11–14) as well as an enrichment of T cells, predominantly T-helper (Th) 1 cells (15) and Th17 cells in adipose tissue (16). Th17 cells are a major source of IL-17 (17), and studies in both obese humans and mice have shown an increase in plasma IL-17 concentrations in obese compared with lean individuals/mice (18, 19).

Recent studies have shown that high sodium intake drives Th17 cell differentiation (20, 21) and thus may exacerbate local or systemic inflammatory conditions. Elevated concentrations of salt may be sensed in the gut, because mice fed a high-salt diet exhibited an increased percentage of $CD4^+$ $IL17^+$ cells in the lamina propria (20), suggesting increased inflammatory immune infiltration in the gut. Experimental models of intestinal inflammation have shown inflammatory changes specific to the mesenteric adipose depot (22). However, a comparative analysis of adipose depots influenced by Th17 cells in HF compared with low-fat (LF) feeding conditions is lacking. Therefore, we evaluated the effects of an HF, high-salt diet on inflammatory responses across different adipose depots in obese mice. Our hypothesis was that the proinflammatory effects of HF feeding would be further exacerbated by the addition of salt to the diet, particularly with respect to the mesenteric depot.

Methods

Animals and diets. All procedures were executed in agreement with the guidelines approved by the US Public Health Service and the Institutional Animal Care and Use Committee at Texas A&M University. Male IL-17 reporter C57BL6 mice (3 mo of age; no. 018472; Jackson Laboratories) were assigned 1 of 4 experimental diets: HF (60% kcal from fat; $n = 7$), HF + high-salt (HF+NaCl; $n = 7$), control (LF; 10% kcal from fat; $n = 7$), or LF + high-salt (LF+NaCl; $n = 6$) for 12 wk. Information on sample size calculation is found in **Supplemental Methods** and **Supplemental References**. All diets were purchased from Research Diets. On the basis of previous reports shown to induce Th17 cell differentiation (20, 21, 23), the high-salt diets contained ~4% wt:wt NaCl, whereas the regular HF and LF diets contained ~0.3% wt:wt NaCl. On the basis of the body surface area normalization method for converting a dose from animals to humans (24), the high-salt group consumed a human equivalent dose of 6.2 g sodium/d. This represents a dose above the average global intake but well within the range of higher intakes reported at >9 g/d (25, 26). The composition and nutritional information of the 4 diets is found in **Supplemental Table 1** and Supplemental References. Body weight and feed intake were monitored weekly. At the end of the treatment period, mice were killed by using carbon dioxide and cervical dislocation. Subsequently, adipose tissue samples were processed immediately for adipose tissue organ culture or snap-frozen and stored at −80°C for further analysis by RNA sequencing as described below.

Adipose tissue morphometry. Additional adipose tissue samples were fixed in 4% paraformaldehyde, paraffin-embedded, and stained with hematoxylin and eosin. Images were captured with a Nikon Cool-SNAP camera and NIS-Elements software. Adipocyte size was quantified with the open-share Fiji program Adiposoft 1.13 (http://fiji.sc/Adiposoft). A continuous block of cells was measured in a 509-mm^2 field to determine average cell size and size distribution for each treatment group.

Serum adipokine profiles. At the time of killing, cardiac blood was collected and allowed to clot at room temperature for 30 min, then centrifuged at 1500 *g* for 15 min, and the serum was stored at −80°C. Serum IL-18 was measured with the Mouse IL18 ELISA Kit (R&D Systems) and renin I with the Mouse Renin I ELISA kit (RayBiotech) on a SpectraMax 190 Microplate Reader (Molecular Devices). Serum concentrations of IL-1β, IL-4, IL-6, IL-17a, IFN-γ, TNF-α, leptin, resistin, and adiponectin were measured by customized Bio-Plex immunoassays on the Bio-Plex 200 System by using Bio-Plex Manager 6.0 software (BioRad).

Adipose tissue organ culture. Subcutaneous (inguinal) and visceral (mesenteric and epididymal) adipose tissue samples (200 mg/depot) were isolated and cultured as previously described (27). The adipose tissue explants (200 g/L) were incubated for 24 h at 37°C in 5% CO_2. As a positive control to show the responsiveness of adipose tissue in organ culture, a subset of epididymal adipose tissue samples were cultured in the presence of 10 μg LPS/mL. After the incubation period, the medium was aspirated from the floating fat and centrifuged for 5 min at 500 *g* at room temperature to remove any excess lipids or debris. The resultant supernatant was separated into aliquots and stored at −80°C until further analysis. Cell culture supernatants were analyzed by the same Bio-Plex immunoassays described above.

RNA isolation and RNA sequencing. RNA was isolated from adipose tissues by using the ToTALLY RNA kit (Ambion) and RNeasy kits (Qiagen). RNA quality was assessed by the Agilent 2100 Bioanalyzer with the use of the Agilent RNA 600 Nano kit, and all samples had an RNA Integrity Number score >8.0. The samples were randomized within tissue type, and sequencing libraries were generated by using the TruSeq RNA Sample Preparation kit (Illumina) as per the manufacturer's instructions. Five microliters of External RNA Controls Consortium standard (LifeTech) was added with the starting RNA at a dilution of 1:1000. Libraries were pooled and sequenced on an Illumina HiSeq 2500 at the Texas AgriLife Genomics and Bioinformatics core facility (College Station, TX). Sequence cluster identification, quality prefiltering, base calling, and uncertainty assessment were performed by using Illumina's HCS 2.2.38 and RTA 1.18.61 software with default parameter settings. Sequencer .bcl basecall files were formatted into .fastq files by using bcl2fastq 1.8.4 script configureBclToFastq.pl. Samples were demultiplexed during the execution of the configureBclToFastq.pl script, except in the case of RAD-Seq or related protocols where known expected sequences (i.e., restriction enzyme sequences) were verified for the purposes of sample demultiplexing. The demultiplexed data were aligned by using STAR with default parameters (28) and referenced against *Mus musculus* [University of California, Santa Cruz (UCSC) version mm10]. Differentially expressed genes were determined by using EdgeR (29) on the basis of the matrix of gene counts. Data are expressed as $\log_2$ fold-changes with corresponding false discovery rate–adjusted *P* values (or *q* values).

Ingenuity Pathway Analyses. Functional analyses of the RNA-sequencing data were performed by using QIAGEN's Ingenuity Pathway Analysis (IPA). To perform IPA analysis, all genes expressed in adipose depots were uploaded and stringency was set at $q < 0.01$ and >2-fold change. Core analysis allowed us to explore the data sets in the context of canonical pathways and upstream regulators that were different between dietary treatments and adipose depots. *P* values were calculated with the right-tailed Fisher's exact test. The *P* value and ratio associated with the canonical pathways and upstream regulators are a measure of their statistical significance with respect to the eligible molecules for the data set and a reference set of molecules.

Statistical analysis. GraphPad Prism 6.0 was used to perform the statistical analyses. Data were analyzed by using a 2-factor ANOVA with

[9] Abbreviations used: *Emr1*, epidermal growth factor-like module containing mucin-like hormone receptor 1; *Foxp3*, forkhead box P3; *Gata3*, GATA binding protein 3; HF, high-fat; HF+NaCl, high-fat + high-salt; IPA, Ingenuity Pathway Analysis; *Itgax*, integrin αX; LF, low-fat; LF+NaCl, low-fat + high-salt; M1, classically activated macrophage; *Mcp1*, monocyte chemotactic protein 1; *Nos2*, NO synthase; *Rorc*, nuclear receptor retinoic acid receptor-related orphan receptor γ; *Stat3*, signal transducer and activator of transcription 3; *Stat4*, signal transducer and activator of transcription 4; *Tbx21*, T-box transcription factor Th, T helper; *Tnf*, tumor necrosis factor.

the main effects of fat and salt. If justified, Bonferroni's multiple-comparisons test was used for post hoc comparisons. Data were tested for normality by the Shapiro-Wilk test. Nonparametric data were analyzed by using the Kruskal-Wallis test, followed, if justified, by Dunn's multiple-comparisons test. In addition, Student's *t* test was used to establish differences relative to the unstimulated control. Differences were considered significant at $P < 0.05$, and all results are reported as means ± SEMs.

Results

High-salt feeding does not exacerbate the HF diet–induced obese phenotype. During the 12-wk dietary intervention, both the HF and HF+NaCl mice gained more weight than the LF diet–fed mice; however, by 3 wk, the HF group weighed significantly more than the HF+NaCl group ($P < 0.05$) (**Figure 1**A). Total food intake by weight for the 12-wk period did not differ between any of the groups (LF = 245 ± 9.1, LF+NaCl = 258 ± 16.7, HF = 232 ± 7.9, and HF+NaCl = 237 ± 10.4 g); however, the HF diets were more energy dense than the LF diets (Supplemental Table 1), resulting in a greater overall caloric intake by the HF groups than in the LF groups (LF = 931 ± 34.6, LF+NaCl = 955 ± 61.8, HF = 1206 ± 41.1, and HF+NaCl = 1185 ± 52.0 kcal/12 wk). The addition of salt to either the LF or HF diets did not influence adipose mass in the subcutaneous or mesenteric depots (Figure 1B). In contrast, the HF+NaCl diet–fed mice had a greater epididymal adipose tissue mass than did the HF diet–fed mice ($P < 0.01$) (Figure 1B). Compared with the LF groups, the HF and HF+NaCl groups showed greater subcutaneous adipocyte size ($P < 0.05$) (Figure 1C, D) and a shift in adipocyte size distribution, with a greater proportion of adipocytes >10,000 μm^2 (**Supplemental Figure 1**A). Mesenteric adipocyte size was greater in the HF group than in all other groups ($P < 0.01$), and the changes in adipocyte size were characterized by a greater proportion of adipocytes >20,000 μm^2 (Supplemental Figure 1B). The effects of the high-salt diet were most profound in the epididymal adipose depot, with a significantly larger mean adipocyte size (Figure 1F), fewer small adipocytes (<1000 μm^2) ($P < 0.01$), and a much greater number of adipocytes >10,000 μm^2 compared with all other diets ($P < 0.01$) (Supplemental Figure 1C). Although the effects of the high-salt diet on adipocyte size were opposite in the epididymal and mesenteric depots with HF feeding, the interaction term for the fat and salt effect was significant in both depots, indicating that sodium had opposite effects on visceral adipocyte size depending on the fat content of the diet ($P < 0.05$).

Changes in systemic adipokines and cytokines were characterized to evaluate the influence of high-salt feeding on the obese phenotype (**Table 1**). At week 12, mice fed the HF diet had lower concentrations of serum adiponectin and higher concentrations of serum IL-17a, TNF-α, IFN-γ, and leptin than mice fed the LF diet ($P < 0.05$). Including the high amount of salt to the HF diet did not further augment these systemic markers; in fact, in some cases it improved the serum markers of the obese phenotype. This was particularly true for adiponectin concentrations, where the HF+NaCl group had significantly higher concentrations than the HF group ($P < 0.05$). The interaction term for the fat and salt effect was significant, indicating that sodium had opposite effects on adiponectin concentrations depending on the fat content of the diet ($P < 0.01$). The only other variable with a significant interaction term was IL-6 ($P < 0.01$). Compared with mice fed the HF diet, the HF+NaCl group had lower serum concentrations of renin, an enzyme involved in the regulation of blood pressure ($P < 0.04$) (Table 1).

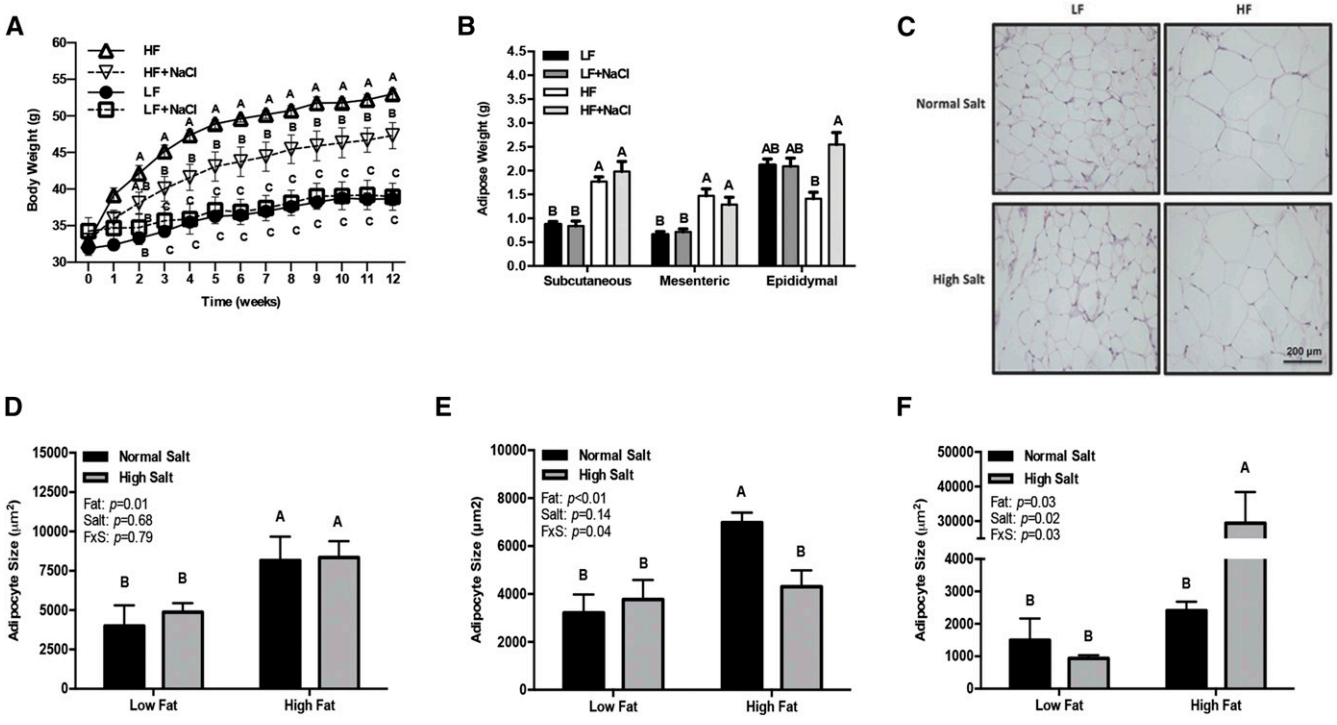

FIGURE 1 Body weight (A), adipose tissue mass (B), representative micrographs of subcutaneous adipose tissue (C), and adipocyte size in subcutaneous (D), mesenteric (E), and epididymal (F) adipose tissue in mice fed 1 of 4 diets containing 2 amounts of salt and fat for 12 wk. Values are means ± SEMs; $n = 6–7$ mice/group (A, B) and $n = 3–4$ mice/group (D–F). Labeled means at a time point without a common letter differ, $P < 0.05$ (A); means within a depot without a common letter differ, $P < 0.05$ (B, D–F). FxS, fat × salt interaction; HF, high-fat; HF+NaCl, high-fat with high-salt; LF, low-fat; LF+NaCl, low-fat with high-salt.

TABLE 1 Serum adipokine and cytokine concentrations in mice fed 1 of 4 diets containing 2 amounts of salt and fat for 12 wk[1]

					P		
	LF	LF+NaCl	HF	HF+NaCl	Fat	Salt	Fat × salt interaction
IL-1β, pg/mL	12.7 ± 6.31	18.8 ± 9.78	16.4 ± 6.77	13.7 ± 5.23	0.48	0.40	0.27
IL-4, pg/mL	118 ± 21.4	157 ± 69.8	200 ± 44.5	216 ± 52.4	0.08	0.28	0.40
IL-6, pg/mL	103 ± 25.3	167 ± 16.1	167 ± 37.1	124 ± 15.3	0.36	0.36	0.04
IL-17a, ng/mL	1.71 ± 0.32^{b}	1.38 ± 0.33^{b}	2.76 ± 0.40^{a}	2.08 ± 0.36^{a,b}	0.02	0.10	0.33
IL-18, pg/mL	275 ± 11.2	278 ± 14.2	260 ± 1.80	260 ± 7.29	0.05	0.44	0.42
TNF-α, pg/mL	7.46 ± 1.17^{b}	11.1 ± 2.42^{a,b}	15.9 ± 2.11^{a}	16.5 ± 3.79^{a}	0.01	0.22	0.29
IFN-γ, pg/mL	479 ± 106^{b}	565 ± 96.7^{a,b}	906 ± 61.6^{a}	723 ± 96.9^{a,b}	<0.01	0.31	0.09
Resistin, ng/mL	57.6 ± 9.79	38.8 ± 27.3	73.3 ± 21.3	59.9 ± 12.4	0.16	0.19	0.44
Leptin, ng/mL	28.3 ± 3.23^{b,c}	20.7 ± 3.88^{c}	64.5 ± 2.83^{a}	60.5 ± 5.72^{a,b}	<0.01	0.10	0.34
Adiponectin, μg/mL	7.63 ± 0.32^{a}	6.67 ± 0.31^{a,b}	5.54 ± 0.33^{b}	6.83 ± 0.38^{a,b}	<0.01	0.31	<0.01
Renin I, ng/mL	1.29 ± 0.18^{a,b}	1.00 ± 0.15^{a,b}	1.53 ± 0.28^{a}	0.83 ± 0.10^{b}	0.44	0.02	0.29

[1] Values are means ± SEMs, n = 6–7 mice/group. Labeled means in a row without a common superscript letter differ, $P < 0.05$. HF, high-fat; HF+NaCl, high-fat with high-salt; LF, low-fat; LF+NaCl, low-fat with high-salt.

Adipose tissue function is impaired by HF feeding in select depots. Adipose tissue functions as an endocrine organ, secreting a wide range of adipokines. We therefore characterized changes in the secretion of select adipokines across different adipose depots after the consumption of an HF diet (**Figure 2**). There was a significant effect of fat on adiponectin secretion in all depots ($P < 0.01$) and no effect of salt ($P = 0.29$) (Figure 2A). In contrast, leptin secretion was different in all 3 adipose depots. In the subcutaneous depot, leptin secretion was unaltered by diet, whereas in the mesenteric adipose depot leptin secretion was greater in the HF diet–fed mice than in the LF group ($P < 0.05$) and in the epididymal depot leptin secretion was less in HF diet–fed mice than in the LF group ($P < 0.01$) (Figure 2B). Resistin secretion from the HF group was significantly less than in the LF group across all depots ($P < 0.05$), and the addition of a high amount of salt did not further influence resistin secretion (Figure 2C). In the epididymal adipose depot, secretion of the inflammatory cytokine IL-6 was greater with HF feeding than with LF feeding ($P < 0.01$). In the subcutaneous depot, IL-6 secretion in the HF group was greater than in the HF+NaCl group ($P = 0.05$) (Figure 2D). There was no interaction between fat and salt observed for the secretion of adiponectin, leptin, resistin, or IL-6. All of the other cytokines examined were below the level of detection under basal conditions (**Supplemental Figure 2**A). However, in the presence of LPS, concentrations of IL-17, IL-1β, and IFN-γ secreted from epididymal adipose tissue were detected (Supplemental Figure 2A), suggesting that the organ culture model was responsive to stimuli but unaltered by dietary intervention (Supplemental Figure 2B).

RNA sequencing reveals depot-specific responsiveness to diet. Functional gene set enrichment analysis was performed by using IPA pathway profiling to probe the biological relevance of the differentially expressed genes between diets and adipose depots. The top conical pathways and upstream regulators altered by the group fed the HF diet compared with those fed LF (control) diet in distinct adipose depots are reported in **Supplemental Table 2**. The results show activation of several pathways involving immune cell regulation/response, particularly in the subcutaneous depot with HF feeding.

Immune cell recruitment in response to HF feeding has been documented in epididymal adipose tissue (15). Therefore, we used the RNA-sequencing data to further characterize the immunologic status of different adipose depots after dietary intervention. Fold-changes in the selected adipokines in the LF +NaCl, HF, and HF+NaCl diet–fed groups relative to the LF diet–fed group are shown in **Supplemental Table 3**. We observed that most changes in gene expression were in mice fed the HF diet compared with all other groups, particularly in the subcutaneous and mesenteric depots (Supplemental Table 3). In general, the secretory pattern of resistin in different adipose depots in response to the HF diet (Figure 2) was comparable to the RNA gene expression data (Supplemental Table 3). However, there was little association between circulating concentrations of inflammatory mediators (Table 1) and gene expression (Supplemental Table 3) in the selected adipose depots. These data suggest that there may be other depots or tissues contributing to the systemic low-grade chronic inflammation observed after HF feeding.

A significant increase in the macrophage marker epidermal growth factor-like module containing mucin-like hormone receptor 1 (*Emr1*) in response to HF feeding was observed in all 3 adipose depots (Supplemental Table 3). In addition, the increase in *Emr1* was mirrored by a significant upregulation of the M1 marker integrin αX (*Itgax*) in all 3 depots of HF-fed mice (Supplemental Table 3). The RNA-sequencing results for the Th1, Th2, Th17, and regulatory T cell markers exhibited a less distinctive pattern and varied between depots (Supplemental Table 3). In the epididymal adipose depot, the HF diet did not significantly alter T cell markers examined, but differing effects were noted in the subcutaneous and mesenteric depots (Supplemental Table 3). In the subcutaneous depot, signal transducer and activator of transcription 4 (*Stat4*), T-box transcription factor (*Tbx21*), GATA binding protein 3 (*Gata3*), *Il21*, and forkhead box P3 (*Foxp3*) were upregulated in the HF group compared with the LF group (Supplemental Table 3). In contrast, in the mesenteric depot, *Stat4* was upregulated, whereas *IL21,* nuclear receptor retinoic acid receptor-related orphan receptor γ (*Rorc*), and *Foxp3* were downregulated in the HF group compared with the LF group (Supplemental Table 3).

Because changes in the M1 macrophage marker *Itgax* with HF compared with LF feeding were observed in all adipose tissues, we used IPA to further examine genes associated with this marker. Pathway analysis of *Itgax* gene interactions in adipose tissues of HF relative to LF diet–fed mice is shown in **Figure 3**. Intriguingly, even though *Itgax* was upregulated in all depots, the surrounding networks did not show the same degree of activation. Many genes of the regulatory network involving

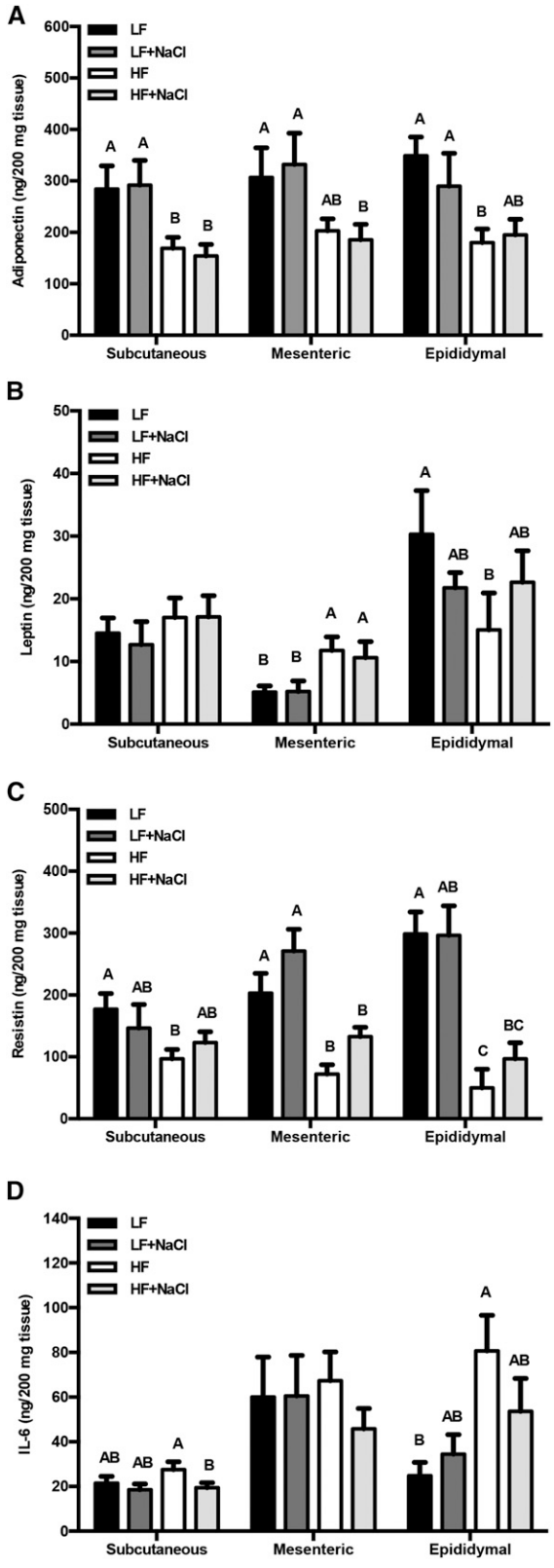

FIGURE 2 Secreted concentrations of adiponectin (A), leptin (B), resistin (C), and IL-6 (D) in media of adipose tissue organ cultures from mice fed 1 of 4 diets containing 2 amounts of salt and fat for 12 wk. Values are means ± SEMs, n = 6–7 mice/group. Labeled means within a depot without a common letter differ, $P < 0.05$. HF, high-fat; HF+NaCl, high-fat with high-salt; LF, low-fat; LF+NaCl, low-fat with high-salt.

Itgax were upregulated in the subcutaneous depot, whereas little change and, in some cases, downregulation of pathway genes were noted in the epididymal and mesenteric depots, respectively (Figure 3).

Discussion

The lack of successful therapeutic treatments for the current obesity epidemic emphasizes the need for a greater understanding of the basic biology of the disease and how the organ systems involved respond differently to pharmacologic and dietary interventions. Adipose tissue is one of the major organs that undergo severe remodeling and functional changes during the onset of obesity. Gene expression profile studies in humans (3, 30–32) have indicated clear differences between visceral and subcutaneous adipose depots. More recently, data from murine models indicated that the composition of different intra-abdominal visceral depots is unique (5). Thus, the current study extends the present state of knowledge by characterizing the response of distinct adipose depots to different dietary factors. We induced obesity by using an HF diet, which has been previously shown to increase serum TNF-α, IL-17, and leptin concentrations (18, 33, 34), in combination with a high-salt diet, which has been shown to induce proinflammatory Th17 cells (20, 21), to examine depot-specific changes in adipose tissue function.

More than 15 y ago, Montague et al. (3) explored site-related differences in human adipocyte leptin expression and showed that leptin mRNA appeared to be expressed predominantly in subcutaneous adipocytes instead of omental adipocytes. A short time after this, Gottschling-Zeller et al. (35) showed that leptin secretion from subcutaneous adipose was 3-fold higher relative to omental adipocytes. We observed an increase in leptin secretion from the mesenteric adipose tissue in response to HF feeding; however, this observation did not hold true for the other visceral depot examined (epididymal) and there was no effect of diet on the subcutaneous depot (Figure 2). Previous work in human adipocytes showed that adiponectin released by omental and subcutaneous adipocytes was similar in lean and obese individuals. However, adiponectin released by omental adipocytes from obese individuals was significantly reduced, whereas that of subcutaneous adipocytes was not affected (36). Consistent with these findings, we showed that the secretion of some adipokines, such as adiponectin and resistin, was altered similarly across multiple depots but others (e.g., leptin and IL-6) appear to be depot-specific (Figure 2). The exact mechanism for these depot-specific differences is unknown; however, there are histologic and gene expression differences across depots. Consistent with previous reports (37), data from the current study show divergent effects of diet-induced obesity on adipocyte size in the epididymal, mesenteric, and subcutaneous adipose depots. Furthermore, reported differences in lipogenic genes suggest that the epididymal adipose depot has lower metabolic activity and is less responsive to HF feeding than the subcutaneous or other visceral depots (37, 38), and thus the structure and functional differences in depots may be contributing to some of the depot-specific differences observed in the current study.

It is thought that part of the chronic inflammation observed in obesity is due to immune cell infiltration and altered production of adipokines (2, 39). By performing comparative fluorescence-activated cell sorting analysis of immune cells across adipose depots, recent studies have expanded our understanding of how distinct adipose depots mediate disease

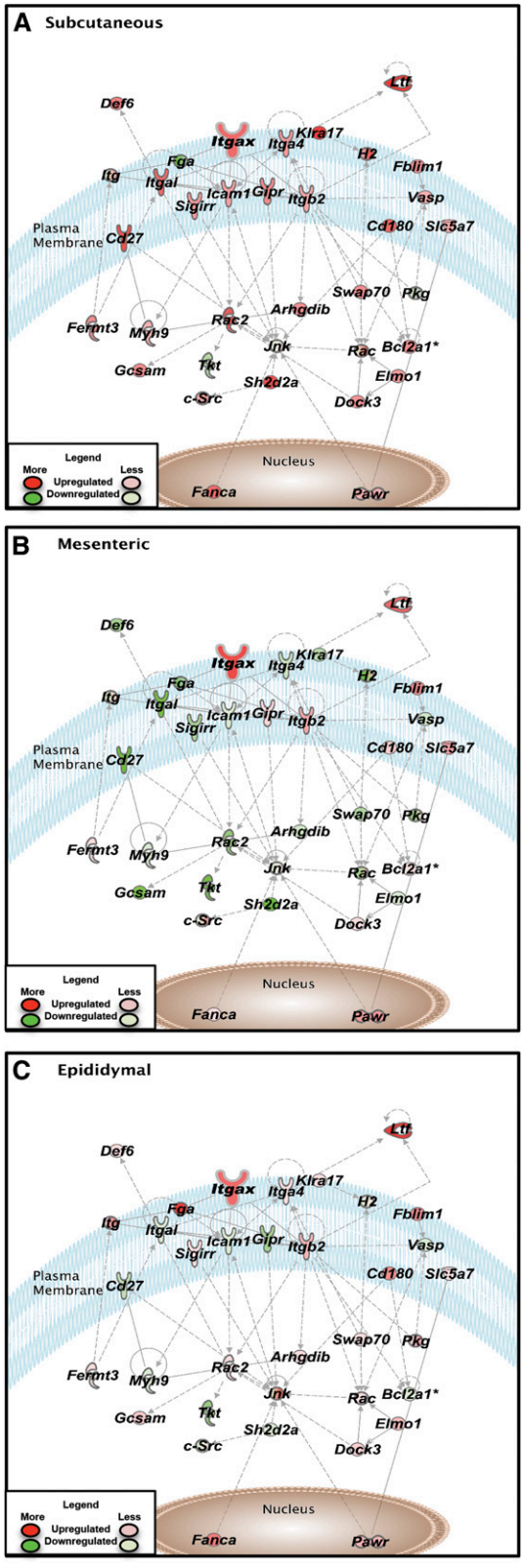

FIGURE 3 Genetic networks generated from the differentially expressed genes from adipose tissues of mice fed a LF or a HF diet for 12 wk. The Ingenuity Pathway Analysis–generated networks of genes associated with *Itgax* signaling in subcutaneous (A), mesenteric (B), and epididymal (C) adipose tissue are shown. The solid and dotted lines between genes represent a direct and indirect relation, respectively. The intensity of the node color indicates the expression level of genes, with red representing upregulation and green downregulation in the HF group relative to the LF group (n = 5 mice/group). Asterisks

progression (5). Specifically, global differences in immune cell populations from the stromal vascular fraction of 3 different adipose depots (parametrial, retroperitoneal, and omental) were reported. However, this study was conducted in lean mice and showed differences in the microenvironments, more specifically enrichment of leukocyte populations (specifically T cells) within the omental depot compared with the parametrial or retroperitoneal depots. The current study adds to previous research by providing insight into changes in the adipose microenvironment that occur with diet-induced obesity (Supplemental Tables 2 and 3).

Adipose tissue macrophage numbers increase in obesity in multiple adipose depots, such as perigonadal, perirenal, mesenteric, and subcutaneous depots (40). A strong correlation between adipocyte size and macrophage infiltration has been reported, with the strongest correlation being observed in the mesenteric depot and the weakest in the subcutaneous depot (40). Furthermore, it is known that diet-induced obesity decreases the expression of genes characteristic of M2 or "alternatively activated" macrophages and increases the expression of genes encoding *Tnf*α and inducible NO synthase (*Nos2*) that are characteristic of M1 or "classically activated" macrophages (13). In the current study, increased expression of the macrophage marker *Emr1* and the M1 marker *Itgax* was observed in all depots after HF feeding (Supplemental Table 3). Additional M1 markers were upregulated in the subcutaneous and epididymal depots after HF feeding; however, the pattern was less consistent across depots.

The enrichment of T cell populations, predominantly the Th1 cell subset, has also been observed in diet-induced obesity; however, there are discrepancies regarding how long after initiation of HF feeding these changes actually occur (15, 41–43). In general, these studies focused primarily on epididymal adipose tissue, raising the possibility that specific depots may display differential expression of immune cell markers during HF feeding. We explored this prospect in the subcutaneous and 2 visceral depots. Our data indicate an upregulation of Th1 cell markers in the subcutaneous depots, a pattern that was not observed in the epididymal or mesenteric depots (Supplemental Table 3). Differences in the duration of our study compared with previous reports on visceral adipose tissue may be an important factor that contributes to the divergent depot effects observed. It has been reported that increases in macrophages occur after ~6–12 wk with HF feeding, whereas increases in lymphocytes occur

(*) indicate the multiple identifiers in the dataset file map to a single change in the IPA Global Molecular Network. *Arhgdib*, ρ guanosine diphosphate dissociation inhibitor β; *Bcl2a1a*, B-cell leukemia/lymphoma 2 related protein A1a; *Cd180*, CD 180; *Cd27*, CD 27; *Def6*, DEF6, guanine nucleotide exchange factor; *Dock3*, dedicator of cyto-kinesis 3; *Elmo1*, engulfment and cell motility 1; *Fanca*, fanconi anemia, complementation group A; *Fblim1*, filamin binding LIM protein 1; *Fermt3*, fermitin family member 3; *Fga*, fibrinogen α chain; *Gcsam*, germinal center-associated, signaling and motility; *Gipr*, gastric inhibitory polypeptide receptor; *H2*, histocompatibility-2, MHC; HF, high-fat; *Icam1*, intercellular adhesion molecule 1; *Itg*, integrin; *Itga4*, integrin α4; *Itgal*, integrin αL; *Itgax*, integrin αX; *Itgb2*, integrin β2; *Jnk*, mitogen-activated protein kinase; *Klra17*, killer cell lectin-like receptor, subfamily A, member 17; LF, low-fat; *Ltf*, lactotransferrin; *Myh9*, myosin, heavy chain 9; *Pawr*, proapoptotic WT1 regulator; *Rac2*, RAS-related C3 botulinum substrate 2; *Sh2d2a*, SH2 domain containing 2A; *Sigirr*, single immunoglobulin and toll-interleukin 1 receptor domain; *Slc5a7*, solute carrier family 5 member 7; *Swap70*, SWA-70protein; *Tkt*, transketolase; *Vasp*, vasodilator-stimulated phosphoprotein.

as early as 2–6 wk or as late as 20–22 wk (14, 15, 41, 42). These depot-specific effects as well as the timing of shifts in immune cell populations should be considered in future studies.

Reports indicate an association between obesity and Th17 cells (18, 19, 44–49). A link between obesity and the increase in plasma IL-17 concentrations in both HF diet–fed mice (23% fat for 8 wk) and obese women [BMI (in kg/m^2): 30–48] has been documented (18, 19). Similarly, there have been reports of increased Th17 cell phenotype in the adipose tissue, liver, and spleen of obese humans and mice (44–49). However, results are inconsistent, likely due to varying study durations and diet compositions and the contribution of IL-17 across several different tissues in animal models has not been reported. Thus, we investigated the changes in Th17 phenotype in a diet- and depot- specific manner. We observed very low amounts of IL-17 secretion from subcutaneous, epididymal, and mesenteric depots as well as inconsistent gene expression of Th17 cell markers *Il17a*, *Rorc*, signal transducer and activator of transcription 3 (*Stat3*), and *Il21* (Supplemental Table 3). Methodologic differences in the type of samples analyzed (mixed cell compared with purified cell populations), basal concentrations compared with ex vivo stimulation, and the use of cell surface markers compared with secreted proteins or gene expression data may account for reported differences. For example, leukocyte subsets isolated from subcutaneous adipose tissue of HF diet–fed mice (60% fat for 18 wk) that were stimulated with phorbol myristate acetate and ionomycin exhibited increased *Il17* expression (46). In a complementary study, CD4$^+$ T cells from the adipose tissue of metabolically abnormal humans expanded in culture exhibited a predominant Th17 and Th22 phenotype (47). Therefore, it is possible that the Th17 response is minimal under normal obese conditions and that T cells of the inflamed obese adipose tissue may be primed or preconditioned to respond to additional stimuli, placing the obese individual at increased risk of an abnormal immune response. Moreover, we must also acknowledge that the increase in *Il17* observed in obese models may originate from other organ and/or tissue sources. For example, hepatic *Il17* mRNA expression was elevated in humans with nonalcoholic steatohepatitis compared with healthy controls and a higher percentage of IL17$^+$ cells was also observed in hepatic mononuclear cells from mice fed an HF diet (59% from fat) for 8 wk (48).

In recent publications, investigators linked high amounts of salt with increased Th17 cell polarization (20, 21). In particular, it was reported that high-salt–fed mice exhibited an increased percentage of CD4$^+$IL17$^+$ cells in the lamina propria (20). Lymph nodes within the lamina propria are a rich source of T cells, and studies have shown that HF feeding causes bacteria from the intestine to translocate into the mesenteric adipose tissue, resulting in adipose tissue inflammation (36, 37). Thus, we hypothesized that the mesenteric adipose depot would be most responsive to high-salt feeding and perhaps further exacerbate the HF phenotype. Surprisingly, we found minimal effect of high-salt feeding on circulating IL-17 concentrations (Table 1), IL-17 secretion (Supplemental Figure 2), and gene expression in adipose depots (Supplemental Table 3). Nevertheless, we observed an increase in the secretion of IL-17 from epididymal adipose tissue with acute LPS stimulation in culture (Supplemental Figure 2). Thus, future studies should not only consider depot-specific effects but also the exposure time (acute compared with chronic) of shifts in immune cell populations. In addition, we must recognize that, although the HF+NaCl group had greater body weights than the LF group, they also had lower body weights than the HF group (Figure 1), which may have contributed to the minimal impact observed on the inflammatory profile. The difference in body weight between the HF and HF+NaCl groups could not be accounted for by differences in adipose mass of the depots investigated; however, the differences in body weight may be attributed to changes in other depots or, as recent research suggests, an association between dietary salt and sarcopenic obesity (50).

In conclusion, our results show differences in response to HF feeding among distinct adipose depots and that the addition of a high-salt diet does little to further exacerbate the inflammatory profile observed in diet-induced obesity (Figures 1 and 2). Furthermore, the current study complements recent data in lean mice, emphasizing the importance of specific visceral depots (5), and clearly showed that different visceral depots from obese mice uniquely respond to dietary interventions (Figures 1–3, Supplemental Figure 1, Supplemental Tables 2 and 3). Thus, special consideration should be given when selecting depots to study the effects of therapeutic interventions on adipose tissue function or basic adipocyte biology as it relates to obesity.

Acknowledgments

We thank Laurie Davidson and Yang-Yi Fan for technical assistance, Evelyn Callaway for technical assistance and mouse breeding, and Roger Zoh for statistical assistance. VCD, DNM, and RSC designed the research; VCD and JSG conducted the research; VCD analyzed the data and performed the statistical analysis; and VCD and RSC wrote the manuscript and had primary responsibility for the final content. All authors read and approved the final manuscript.

References

1. Johnson AR, Milner JJ, Makowski L. The inflammation highway: metabolism accelerates inflammatory traffic in obesity. Immunol Rev 2012;249:218–38.
2. Karastergiou K, Mohamed-Ali V. The autocrine and paracrine roles of adipokines. Mol Cell Endocrinol 2010;318:69–78.
3. Montague CT, Prins JB, Sanders L, Zhang J, Sewter CP, Digby J, Byrne CD, O'Rahilly S. Depot-related gene expression in human subcutaneous and omental adipocytes. Diabetes 1998;47:1384–91.
4. Linder K, Arner P, Flores-Morales A, Tollet-Egnell P, Norstedt G. Differentially expressed genes in visceral or subcutaneous adipose tissue of obese men and women. J Lipid Res 2004;45:148–54.
5. Cohen CA, Shea AA, Heffron CL, Schmelz EM, Roberts PC. Intra-abdominal fat depots represent distinct immunomodulatory microenvironments: a murine model. PLoS One 2013;8:e66477.
6. Yi SS, Kansagra SM. Associations of sodium intake with obesity, body mass index, waist circumference, and weight. Am J Prev Med 2014;46: e53–5.
7. Yi SS, Firestone MJ, Beasley JM. Independent associations of sodium intake with measures of body size and predictive body fatness. Obesity (Silver Spring) 2015;23:20–3.
8. Song HJ, Cho YG, Lee HJ. Dietary sodium intake and prevalence of overweight in adults. Metabolism 2013;62:703–8.
9. Zhou X, Zhang L, Ji WJ, Yuan F, Guo ZZ, Pang B, Luo T, Liu X, Zhang WC, Jiang TM, et al. Variation in dietary salt intake induces coordinated dynamics of monocyte subsets and monocyte-platelet aggregates in humans: implications in end organ inflammation. PLoS One 2013;8:e60332.
10. Baudrand R, Lian CG, Lian BQ, Ricchiuti V, Yao TM, Li J, Williams GH, Adler GK. Long-term dietary sodium restriction increases adiponectin expression and ameliorates the proinflammatory adipokine profile in obesity. Nutr Metab Cardiovasc Dis 2014;24:34–41.
11. Strissel KJ, Stancheva Z, Miyoshi H, Perfield JW II, DeFuria J, Jick Z, Greenberg AS, Obin MS. Adipocyte death, adipose tissue remodeling, and obesity complications. Diabetes 2007;56:2910–8.
12. Lumeng CN, Bodzin JL, Saltiel AR. Obesity induces a phenotypic switch in adipose tissue macrophage polarization. J Clin Invest 2007;117:175–84.

13. Lumeng CN, Deyoung SM, Bodzin JL, Saltiel AR. Increased inflammatory properties of adipose tissue macrophages recruited during diet-induced obesity. Diabetes 2007;56:16–23.
14. Amano SU, Cohen JL, Vangala P, Tencerova M, Nicoloro SM, Yawe JC, Shen Y, Czech MP, Aouadi M. Local proliferation of macrophages contributes to obesity-associated adipose tissue inflammation. Cell Metab 2014;19:162–71.
15. Strissel KJ, DeFuria J, Shaul ME, Bennett G, Greenberg AS, Obin MS. T-cell recruitment and Th1 polarization in adipose tissue during diet-induced obesity in C57BL/6 mice. Obesity (Silver Spring) 2010;18:1918–25.
16. Chen Y, Tian J, Tian X, Tang X, Rui K, Tong J, Lu L, Xu H, Wang S. Adipose tissue dendritic cells enhances inflammation by prompting the generation of Th17 cells. PLoS One 2014;9:e92450.
17. Harrington LE, Hatton RD, Mangan PR, Turner H, Murphy TL, Murphy KM, Weaver CT. Interleukin 17-producing CD4+ effector T cells develop via a lineage distinct from the T helper type 1 and 2 lineages. Nat Immunol 2005;6:1123–32.
18. Shankar E, Vykhovanets EV, Vykhovanets OV, Maclennan GT, Singh R, Bhaskaran N, Shukla S, Gupta S. High-fat diet activates pro-inflammatory response in the prostate through association of Stat-3 and NF-kappaB. Prostate 2012;72:233–43.
19. Sumarac-Dumanovic M, Stevanovic D, Ljubic A, Jorga J, Simic M, Stamenkovic-Pejkovic D, Starcevic V, Trajkovic V, Micic D. Increased activity of interleukin-23/interleukin-17 proinflammatory axis in obese women. Int J Obes (Lond) 2009;33:151–6.
20. Wu C, Yosef N, Thalhamer T, Zhu C, Xiao S, Kishi Y, Regev A, Kuchroo VK. Induction of pathogenic TH17 cells by inducible salt-sensing kinase SGK1. Nature 2013;496:513–7.
21. Kleinewietfeld M, Manzel A, Titze J, Kvakan H, Yosef N, Linker RA, Muller DN, Hafler DA. Sodium chloride drives autoimmune disease by the induction of pathogenic TH17 cells. Nature 2013;496:518–22.
22. Mustain WC, Starr ME, Valentino JD, Cohen DA, Okamura D, Wang C, Evers BM, Saito H. Inflammatory cytokine gene expression in mesenteric adipose tissue during acute experimental colitis. PLoS One 2013;8:e83693.
23. Monk JM, Hou TY, Turk HF, Weeks B, Wu C, McMurray DN, Chapkin RS. Dietary n-3 polyunsaturated fatty acids (PUFA) decrease obesity-associated Th17 cell-mediated inflammation during colitis. PLoS One 2012;7:e49739.
24. Reagan-Shaw S, Nihal M, Ahmad N. Dose translation from animal to human studies revisited. FASEB J 2008;22:659–61.
25. Powles J, Fahimi S, Micha R, Khatibzadeh S, Shi P, Ezzati M, Engell RE, Lim SS, Danaei G, Mozaffarian D; Global Burden of Diseases Nutrition and Chronic Diseases Expert Group (NutriCoDE). Global, regional and national sodium intakes in 1990 and 2010: a systematic analysis of 24 h urinary sodium excretion and dietary surveys worldwide. BMJ Open 2013;3:e003733.
26. Zhu H, Pollock NK, Kotak I, Gutin B, Wang X, Bhagatwala J, Parikh S, Harshfield GA, Dong Y. Dietary sodium, adiposity, and inflammation in healthy adolescents. Pediatrics 2014;133:e635–42.
27. Thalmann S, Juge-Aubry CE, Meier CA. Explant cultures of white adipose tissue. Methods Mol Biol 2008;456:195–9.
28. Dobin A, Davis CA, Schlesinger F, Drenkow J, Zaleski C, Jha S, Batut P, Chaisson M, Gingeras TR. STAR: ultrafast universal RNA-seq aligner. Bioinformatics 2013;29:15–21.
29. Robinson MD, McCarthy DJ, Smyth GK. edgeR: a Bioconductor package for differential expression analysis of digital gene expression data. Bioinformatics 2010;26:139–40.
30. Spoto B, Di Betta E, Mattace-Raso F, Sijbrands E, Vilardi A, Parlongo RM, Pizzini P, Pisano A, Vermi W, Testa A, et al. Pro- and anti-inflammatory cytokine gene expression in subcutaneous and visceral fat in severe obesity. Nutr Metab Cardiovasc Dis 2014;24:1137–43.
31. Korsic M, Gotovac K, Nikolac M, Dusek T, Skegro M, Muck-Seler D, Borovecki F, Pivac N. Gene expression in visceral and subcutaneous adipose tissue in overweight women. Front Biosci (Elite Ed) 2012;4: 2834–44.
32. Lefebvre AM, Laville M, Vega N, Riou JP, van Gaal L, Auwerx J, Vidal H. Depot-specific differences in adipose tissue gene expression in lean and obese subjects. Diabetes 1998;47:98–103.
33. Maffei M, Halaas J, Ravussin E, Pratley RE, Lee GH, Zhang Y, Fei H, Kim S, Lallone R, Ranganathan S. Leptin levels in human and rodent: measurement of plasma leptin and ob RNA in obese and weight-reduced subjects. Nat Med 1995;1:1155–61.
34. Surwit RS, Petro AE, Parekh P, Collins S. Low plasma leptin in response to dietary fat in diabetes- and obesity-prone mice. Diabetes 1997;46:1516–20.
35. Gottschling-Zeller H, Birgel M, Scriba D, Blum WF, Hauner H. Depot-specific release of leptin from subcutaneous and omental adipocytes in suspension culture: effect of tumor necrosis factor-alpha and transforming growth factor-beta1. Eur J Endocrinol 1999;141:436–42.
36. Drolet R, Belanger C, Fortier M, Huot C, Mailloux J, Legare D, Tchernof A. Fat depot-specific impact of visceral obesity on adipocyte adiponectin release in women. Obesity (Silver Spring) 2009;17:424–30.
37. Caesar R, Manieri M, Kelder T, Boekschoten M, Evelo C, Muller M, Kooistra T, Cinti S, Kleemann R, Drevon CA. A combined transcriptomics and lipidomics analysis of subcutaneous, epididymal and mesenteric adipose tissue reveals marked functional differences. PLoS One 2010;5:e11525.
38. Wronska A, Lawniczak A, Wierzbicki PM, Goyke E, Sledzinski T, Kmiec Z. White adipose tissue depot-specific activity of lipogenic enzymes in response to fasting and refeeding in young and old rats. Gerontology 2015;61:448–55.
39. Han JM, Levings MK. Immune regulation in obesity-associated adipose inflammation. J Immunol 2013;191:527–32.
40. Weisberg SP, McCann D, Desai M, Rosenbaum M, Leibel RL, Ferrante AW Jr. Obesity is associated with macrophage accumulation in adipose tissue. J Clin Invest 2003;112:1796–808.
41. Nishimura S, Manabe I, Nagasaki M, Eto K, Yamashita H, Ohsugi M, Otsu M, Hara K, Ueki K, Sugiura S, et al. CD8+ effector T cells contribute to macrophage recruitment and adipose tissue inflammation in obesity. Nat Med 2009;15:914–20.
42. Duffaut C, Zakaroff-Girard A, Bourlier V, Decaunes P, Maumus M, Chiotasso P, Sengenes C, Lafontan M, Galitzky J, Bouloumie A. Interplay between human adipocytes and T lymphocytes in obesity: CCL20 as an adipochemokine and T lymphocytes as lipogenic modulators. Arterioscler Thromb Vasc Biol 2009;29:1608–14.
43. Kintscher U, Hartge M, Hess K, Foryst-Ludwig A, Clemenz M, Wabitsch M, Fischer-Posovszky P, Barth TF, Dragun D, Skurk T, et al. T-lymphocyte infiltration in visceral adipose tissue: a primary event in adipose tissue inflammation and the development of obesity-mediated insulin resistance. Arterioscler Thromb Vasc Biol 2008;28:1304–10.
44. Bertola A, Ciucci T, Rousseau D, Bourlier V, Duffaut C, Bonnafous S, Blin-Wakkach C, Anty R, Iannelli A, Gugenheim J, et al. Identification of adipose tissue dendritic cells correlated with obesity-associated insulin-resistance and inducing Th17 responses in mice and patients. Diabetes 2012;61:2238–47.
45. Winer S, Paltser G, Chan Y, Tsui H, Engleman E, Winer D, Dosch HM. Obesity predisposes to Th17 bias. Eur J Immunol 2009;39:2629–35.
46. Zuniga LA, Shen WJ, Joyce-Shaikh B, Pyatnova EA, Richards AG, Thom C, Andrade SM, Cua DJ, Kraemer FB, Butcher EC. IL-17 regulates adipogenesis, glucose homeostasis, and obesity. J Immunol 2010;185:6947–59.
47. Fabbrini E, Cella M, McCartney SA, Fuchs A, Abumrad NA, Pietka TA, Chen Z, Finck BN, Han DH, Magkos F, et al. Association between specific adipose tissue CD4+ T-cell populations and insulin resistance in obese individuals. Gastroenterology 2013;145:366–74.e1.
48. Tang Y, Bian Z, Zhao L, Liu Y, Liang S, Wang Q, Han X, Peng Y, Chen X, Shen L, et al. Interleukin-17 exacerbates hepatic steatosis and inflammation in non-alcoholic fatty liver disease. Clin Exp Immunol 2011;166:281–90.
49. Farrell GC, Mridha AR, Yeh MM, Arsov T, Van Rooyen DM, Brooling J, Nguyen T, Heydet D, Delghingaro-Augusto V, Nolan CJ, et al. Strain dependence of diet-induced NASH and liver fibrosis in obese mice is linked to diabetes and inflammatory phenotype. Liver Int 2014;34: 1084–93.
50. Huh JH, Lim JS, Lee MY, Chung CH, Shin JY. Gender-specific association between urinary sodium excretion and body composition: analysis of the 2008–2010 Korean National Health and Nutrition Examination Surveys. Metabolism 2015;64:837–44.